EXPERIMENTAL PROGRAM ON DEBRIS REFLOODING (PEARL) RESULTS ON PRELUDE FACILITY

G. Repetto, T. Garcin, S. Eymery, P. March and F. Fichot
Institut de Radioprotection et de Sureté Nucléaire, Cadarache, France
georges.repetto@irsn.fr, thierry.garcin@irsn.fr, philippe.march@irsn.fr,
stephane.eymery@irsn.fr, florian.fichot@irsn.fr

Abstract

The "Institut de Radioprotection et de Sureté Nucléaire" is developing simulation tools to be used in the safety studies, for the optimization of the Severe Accident Management strategy and to assess the probabilities to stop the progress of In-vessel core degradation in a Nuclear Power Plant. The objective of the experimental program PEARL is to extend the validation of debris reflooding models in 2D and 3D situations. The aim is to predict the consequences of the water reflooding of a severely damaged reactor core where a significant part of the core has collapsed and formed a debris bed.

1. Introduction

During a severe accident in a Pressurized Water Reactor (PWR), the core would be progressively damaged. To stop the progression of the accident, water can be injected into the degraded core. The reflooding models used for Loss of Coolant Accident (LOCA) are not applicable in these situations which require extended models ([1] and [2]), based on the description of the core as a porous medium, to be implemented in simulation tools as ICARE/CATHAREV2 and ASTEC.

The objective of the PEARL experimental program [3] (**P**rogramme **E**xpérimental **A**nalytique sur le **R**enoyage de **L**its de débris) conducted by IRSN in the frame of the SARNET2 network of excellence on Severe Accident [4], and also supported by EDF, is to extend the validation of debris reflooding models in 2D and 3D situations [5]. The aim is to predict the consequences of the water reflooding of a severely damaged reactor core where a large part of the core has collapsed and formed a debris bed. This means the prediction of debris coolability, front propagation and steam production during the quenching after the water injection. In the PEARL facility (Figure 1), the debris bed (Ø540mm, h=500mm and 500kg of stainless steel spherical particles) is heated by means of an induction system. A non heated part at the periphery, with larger porosity, is foreseen to simulate a bypass of the degraded zone in the reactor core.

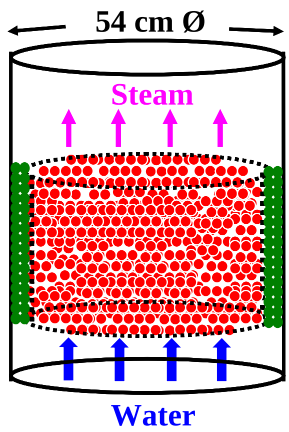

Figure 1 : Debris bed

To reach this objective, a step-wise experimental approach has been adopted consisting in launching a preliminary qualification tests series in a small facility named PRELUDE, to test the performance of the induction heating system and to optimize the instrumentation in a two phase flow (temperature, pressure, water and steam mass flow rates), for a better design of the PEARL facility, to be constructed by IRSN at Cadarache.

Table 1 Experiments on debris bed coolability

Experiments Parameters	Tutu et al BNL (1984)	Dhir et al (1983-1988)	Ginsberg (1986)	SILFIDE EDF (2000)	POMECO RIT	DEBRIS IKE	PRELUDE-IRSN (2009-2011)	PEARL (> 2012)
Reflooding	Bottom flooding	Bottom and Top flooding	Top flooding	Only dry out	Top flooding and dry out	Bottom and Top flooding, dry out	Bottom flooding	Bottom and Top flooding
Temperature (K)	512, 594, 775	875	533 to 977.	Up to 473	Up to 775		Up to 1200	Up to 1300
Pressure (MPa)	0.1	0.1	0.1	0.1	0.1	0.1 to 0.5	0,1 MPa	0.1 to 1MPa (10bar)
Subcooling (K)	0	0 - 75	0	0 - 5	80	80	293 K (room temp.)	0 to 50
Water inlet velocity ($m^3/h/m^2$)	3.6, 7, 16, 26	Gravity driven	Gravity driven	0	Gravity driven with downcomer	1 to 36	2, 5, 10, 20	2 to 50
Heating process	Pre-heated by hot air No power during quench	Induction	Pre-heated by hot air No power during quench	Induction	Internal heaters	Induction	Induction Power maintained during quench (40 to 200W/kg)	Induction Power maintained during quench (100 to 300W/kg)
Geometry Debris mass	 18 kg	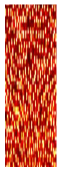 71 kg	 18 kg	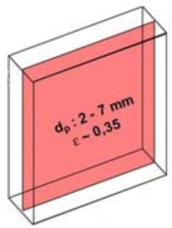	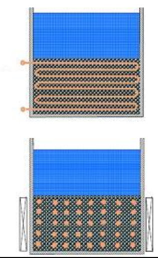	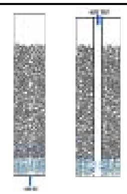 37 kg	bypass 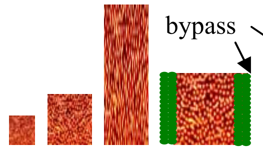 1 2 3 4 5kg 24kg 57kg 58kg	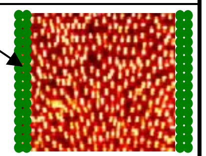 500 kg
Diameter/height	Ø108/422mm	Ø186/550mm	Ø108/422mm	500.600.100mm Parallepipedic geometry	Ø350/450mm	Ø125/640mm Ø150/640mm	1 : Ø110/100mm 2 : Ø180/200mm 3 : Ø180/500mm 4 : Ø290/250mm	Ø540/500mm
Particle diameter (mm)	3.175 (Stainless steel spherical part.)	1.6, 3.2, 6.35	0.89, 3.2, 6.35 and 12.7	2 to 7.2	0.2 to 1	3 to 6 + mixtures and irregular shape	Stainless steel 1, 2, 3 4 + mixtures + non homogeneous size	Stainless steel spherical part. 2, 3 and 4

It is worth to compare our experiments to those already performed or in progress in others experimental programs. Table 1 summarizes some conditions of experiments related to coolability of debris beds (Tutu [6] and Ginsberg [7] at BNL, Wang and Dhir [8] at UCLA, POMECO at RIT [9], SILFIDE at EDF [10], STYX at VTT [11] and DEBRIS at IKE [12]). Important features of PEARL experiments are unique configuration never achieved regarding the scaling (multi-dimensional effects) and the thermal hydraulics conditions (high temperature, high pressure and high power deposition during the reflooding to be representative of the residual power). This paper gives the main features of the first reflooding experimental results obtained in the PRELUDE facility.

2. Description of the PRELUDE facility

PRELUDE facility (Figure 2a) includes several components:

- A water tank for reflooding with water flow measurement,
- A test section varying from Ø110 mm to Ø290 mm containing a debris bed instrumented with thermocouples and pressure sensors,
- An induction furnace (coil around the test device - Figure 2b),
- A downstream heated vertical tube to remove steam from test section, including temperature and steam mass flow rate measurements.

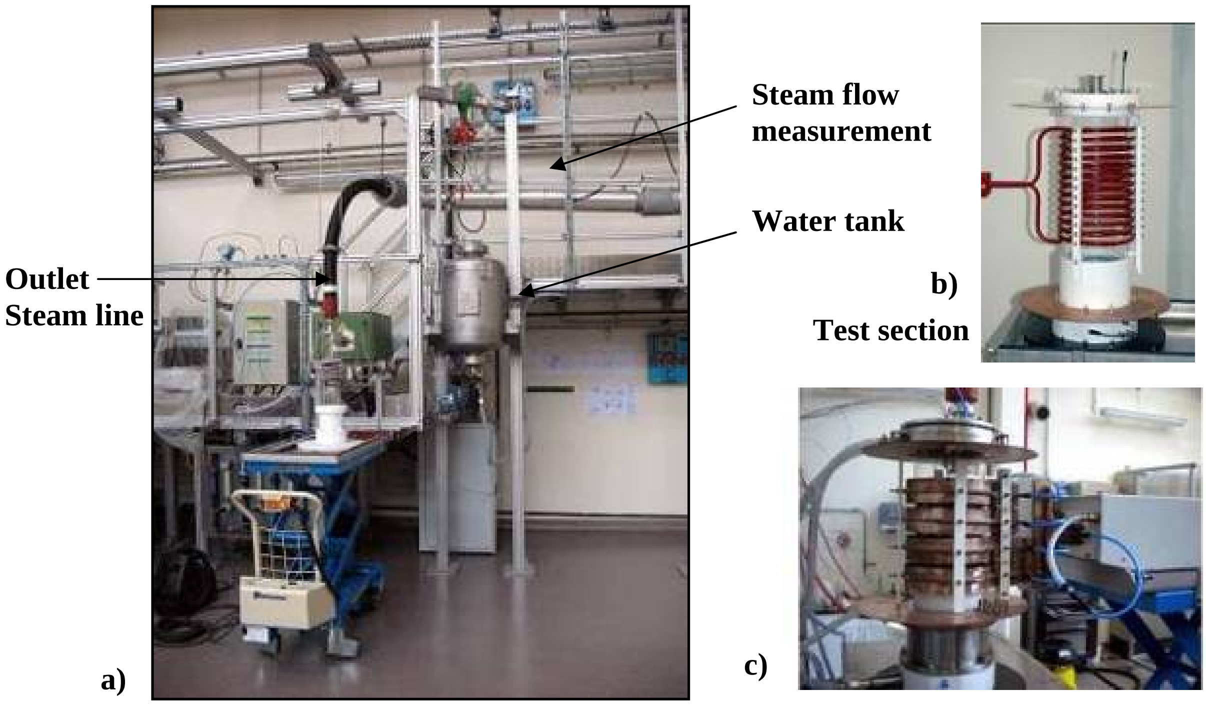

Figure 2: PRELUDE Facility and test section with inductive system

The experimental tests series started using a High Frequency generator (25kW/9-50kHz). In order to increase the power deposition inside the porous medium, in particular for small particles size, a Very High frequency generator (6kW/400kHz) was adopted with slight modification of the inductive coil (circular copper plate illustrated on Figure 2-c).

The debris bed is inserted inside a quartz tube with various possible configurations (Figure 3):

- debris bed (p = 0,400 ± 0,003) with stainless steel balls (d_p = Ø 1, 2, 4, or 8 mm),
- mixed particles (2/4 mm, 4/8mm, etc..) to decrease the porosity (p = 0.376 ± 0.006),
- uniform or non uniform shape of the debris.

The selection of size was made after an extensive review of data including TMI2 debris bed, and experiments like LOFT LP-FP4, PBF SFD-1.4, ISTC 1648, etc [13]. The representation of non spherical fragments by sphere can be taken into account by a modification of the representative average diameter. This point is currently studied by other teams (KTH, IKE) in the frame of SARNET-2 WP5 collaborative project.

The choice of steel particles results from a compromise: on one hand, a metal is needed for induction (and it cannot be a rare and expensive metal) and, on the other hand, it is important to have some similarity of physical properties with UO_2. In the present case, (ρ, Cp) is almost identical for steel and UO_2, which means that the initial stored energy is comparable for both materials. This means that the timing of reflooding and quenching will be comparable. Calculations with both materials have confirmed that assumption [14]. For the biggest particles (4mm), the characteristic time for conduction is 0.3s for the steel particles and 3s for UO2 balls, whereas the average cooling time of a particle is more than 10s: therefore, we can conclude that, in general, the uniformisation of temperature by conduction in the particles will be faster than the decrease of average temperature by cooling, which means that UO2 particles would behave similarly to steel particles. However, near the quench front, where the heat flux is very large, there may be a delay until conduction leads to a uniform temperature in the particles, resulting in a hot central part of the particles while the periphery is quenched. Such effect would be amplified with UO2 particles.

The characterisations of the physical properties of the debris bed (porosity p, permeability, passability..) are obtained with specific experiments (not developed in this paper). Pressure drop measurements with air flow allow the evaluation of coefficients (a and b) in the Ergun correlation type:

$$-\frac{\Delta P}{Z} - \rho_f g = a\,\frac{(1-p)^2}{p^3 d_p^2}\mu_f u_m + b\,\frac{(1-p)}{p^3 d_p}\rho_f u_m^2 \qquad (1)$$

with μ_f *and* ρ_f the dynamic viscosity and the density of the fluid

Ø 2mm **Ø 4mm** **Ø 8mm** **mixed Ø 2/4 mm** **Ø 4/8 mm**

Figure 3 : Debris bed configuration

The stainless steel particles were placed above a debris bed made of quartz particles with diameter Ø 4 mm (Figure 4a) in order to avoid placing a metallic grid which would heat-up because of the induction process.

3. Instrumentation

The major physical variables for model qualification are as follows:

- Water and steam mass flow rate generated during reflooding,
- Temperature of the steam at different points outside the debris bed (type K thermocouples),
- Temperature of the pores inside the debris (thermocouples at different elevations: 10, 50, 100, 150 and 190 mm and radial positions : center, mid radius and periphery – Figure 4a),
- Temperature inside particles of the debris bed (thermocouples with specific development),
- Distribution of the heating power (given by local temperature rise rates – equation (2)),
- Pressure at different points at the boundaries of the debris bed,
- Pressure at several points inside the debris bed (feasibility in progress).

Specific effort has been done on the measurement of the pressure drop across the porous medium during the reflooding (Figure 4b).

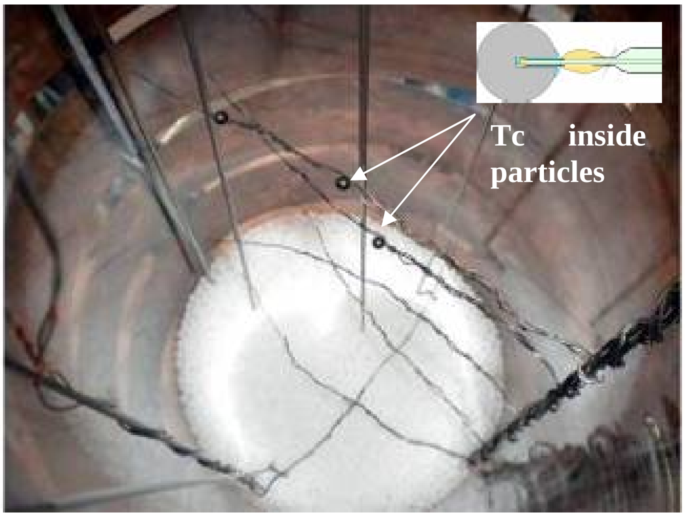

a)

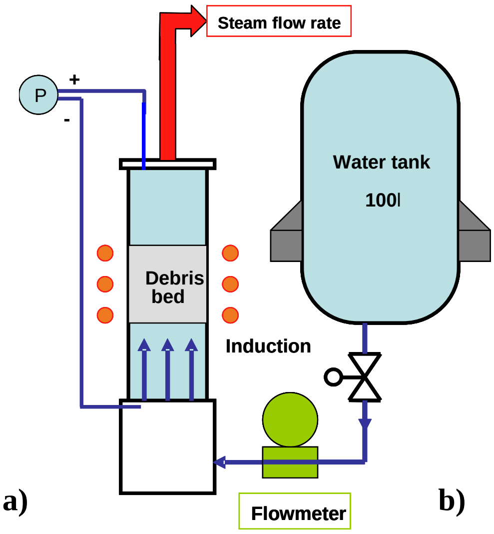

b)

Figure 4 : Instrumentation : thermocouples (left) and pressure drop (right)

The steam mass flow rate is obtained through the measurement of a pressure drop in the outlet circuit.

The power deposition, by means of an electromagnetic induction technology, is evaluated by using the temperature evolution in the various radial and axial location of the thermocouples, during the heat up phase and the heat capacity of the stainless steel (the Cp taken around 500 $kJ.K^{-1}.kg^{-1}$) with the simple relation given below:

$$P(W/kg) = \frac{\partial T}{\partial t} * Cp \qquad (2)$$

The variation of heat capacity does not have a significant impact on reflooding because the global process depends mainly on the initial energy stored in the particles (which depends only on the initial heat capacity and temperature) and the intensity of heat flux which depends very weakly on the heat capacity.

Figure 5 illustrates the rather homogeneous power distribution in the debris bed for Ø4mm particles. Similar distribution is obtained for Ø2mm particles. Nevertheless, the electromagnetic coupling is less efficient, in particular with the Ø1mm particles. The low non-uniformity observed have limited impact reflooding phenomena.

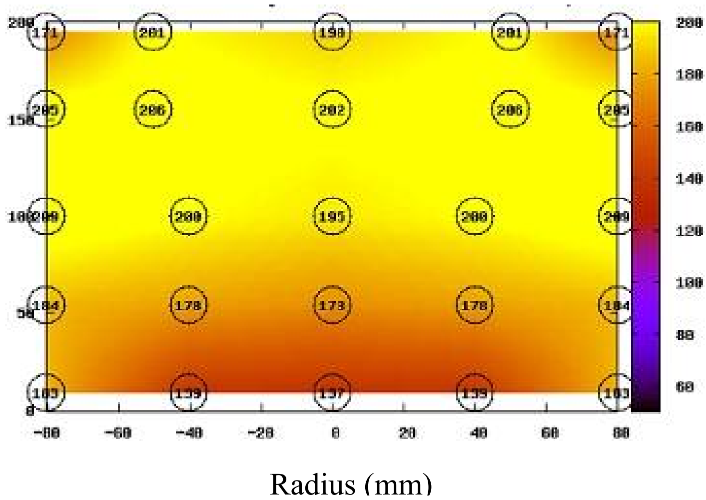

Figure 5: Power distribution (W/kg)

For the test presented in the paper, with an initial temperature of 400°C, the initial enthalpy of the particles is approximately 140 kJ/kg (taking the reference of enthalpy at 100°C). The reflooding takes between 2 and 5 minutes (cf section 5.5), depending on conditions, which corresponds to an additional energy of 24 to 100 kJ/kg, assuming that the volumetric power is 200W/kg. Therefore, the fluctuations, even if they are locally 30% (for the smallest particules), correspond to a local difference of 30 kJ/kg over a total of 240 kJ/kg for the longest reflooding time, i.e. only 15% (locally), which cannot affect significantly the global reflooding phenomena. The impact of non uniformities would be more significant for larger beds, as it is planned for PEARL. Anyway, non uniform power distribution can be characterized before the tests and easily introduced in the calculations in order to take it into account for interpretation.

4. PRELUDE Test matrix

Preliminary reflooding tests were carried out involving a debris bed of Ø4 mm particles inside a 110 mm external diameter, and 100 mm height test section (5 kg), at atmospheric pressure. The range of experimental parameters investigated is:

- Inlet water superficial velocity at 4 to 30 $m^3/h/m^2$, in the range foreseen in the PEARL test matrix,
- Power deposition at 300W/kg (maintained or not during the reflooding phase),
- Initial debris bed temperature before the reflooding at 150, 230, 310°C and 700°C.

This campaign (Table 2) demonstrated the feasibility of reflooding experiments up to 700°C, with variation of mass flow rate due to gravimetric injection.

Table 2 Test matrix – preliminary campaign

Test reference	Temperature	Reflooding water flow rate
110_4_Amb_Renoyage1 *	150°C	~25 $m^3/h/m^2$
110_4_Amb_Renoyage2	220°C	~25 $m^3/h/m^2$
110_4_Amb_Renoyage3	125°C	11 $m^3/h/m^2$
110_4_Amb_Renoyage4	230°C	11 $m^3/h/m^2$
110_4_Amb_Renoyage5	310 °C	6 to 4 m/h
110_4_Amb_Renoyage7	700 °C	10 to 5 m/h

* without power deposition during the reflooding

Jointly, additional heating PRELUDE tests (without reflooding) were performed to evaluate the power distribution inside various debris bed diameters (Ø110 to Ø290mm) using stainless amagnetic steel particles, Ø2, Ø4 and Ø8 mm and mixed particles (Ø2/Ø4 or Ø4/Ø8mm).
The bigger Ø180mm test section diameter includes 24 kg of slightly oxidised Stainless steel Ø4mm particles and needs a high frequency generator (up to 400 kHz) for the inductive furnace to reach the nominal power deposition at about 200W/kg.

The first campaign of reflooding experiments (10 tests), using the Ø180mm test section was performed with the Ø4mm diameter for the particles size. The most significant experiments (Table 3) allowed to test an instrumentation during reflooding in the PRELUDE facility by progressive increase of the initial temperature of the debris (200 to 930°C) and the power deposition in the debris bed (40 to 140W/kg under the nominal value).

Table 3 Test matrix – 1st campaign (particles size of Ø 4 mm)

Test reference	Temperature	Power deposition	Water flow rate
15/16* D180 B4Q4 T200	210 °C	40 W/kg	6 $m^3/h/m^2$
17/20* D180 B4Q4 T400	410 °C	40 W/kg	6 $m^3/h/m^2$
21 D180 B4Q4 T400	420 °C	100 W/kg	6,5 $m^3/h/m^2$
25/26* D180 B4Q4 T400	415 °C	140 W/kg	6,5 $m^3/h/m^2$
29/30* D180 B4Q4 T700	720 °C	140 W/kg	6,5 $m^3/h/m^2$
31 D180 B4Q4 T1000	930 °C	120 W/kg	6 $m^3/h/m^2$

* tests reproduced with same T/H conditions for repeatability to increase the reliability of the measurements

The 2nd campaign (15 tests) was performed for the same debris bed for two temperature levels (400 and 700°C) up to the nominal power deposit: 200W/kg. The most representative conditions are reported in Table 4.

The thermal hydraulics conditions were focussed mainly on the effect of the inlet flow velocity (values foreseen for the large scale PEARL experiments: 2, 5 10 and 20 $m^3/h/m^2$).
The 3rd campaign (10 tests), summarized in Table 5, was performed with smaller particles size (Ø2 mm).

Table 4 Test matrix – 2nd campaign (particles size of Ø 4 mm)

Test reference	Temperature	Power deposition	Water flow rate
46 D180 B4Q4 T700	720 °C	200 W/kg	5 $m^3/h/m^2$
57 D180 B4Q4 T700	720 °C	150 W/kg	2 $m^3/h/m^2$
58/67 D180 B4Q4 T400	410 °C	200 W/kg	2 $m^3/h/m^2$
69/71 D180 B4Q4 T400	430 °C	200 W/kg	5 $m^3/h/m^2$
72/73 D180 B4Q4 T400	405 °C	200 W/kg	10 $m^3/h/m^2$
74/76 D180 B4Q4 T400	415 °C	200 W/kg	20 $m^3/h/m^2$
78 D180 B4Q4 T700	700 °C	200 W/kg	10 $m^3/h/m^2$
79/80 D180 B4Q4 T700	735 °C	200 W/kg	5 $m^3/h/m^2$
81 D180 B4Q4 T700	710 °C	200 W/kg	20 $m^3/h/m^2$

Table 5 Test matrix – 3rd campaign (particles size of Ø 2 mm)

Test reference	Temperature	Power deposition	Water flow rate
87/88 D180 B2Q4 T400	420 °C	175 W/kg	5 $m^3/h/m^2$
90 D180 B2Q4 T700	720 °C	195 W/kg	5 $m^3/h/m^2$
91 D180 B2Q4 T400	420 °C	190 W/kg	2 $m^3/h/m^2$
92 D180 B2Q4 T400	420 °C	190 W/kg	10 $m^3/h/m^2$
94/93* D180 B2Q4 T700	710 °C	60 and 0 W/kg	5 $m^3/h/m^2$
95 D180 B2Q4 T700	710 °C	175 W/kg	10 $m^3/h/m^2$
96 D180 B2Q4 T400	410 °C	0 W/kg	10 $m^3/h/m^2$

* tests reproduced with same thermal hydraulics conditions as for nb 90 but with reduced power during reflooding

The last campaign was performed with the smallest particle size of Ø1mm (Table 6). In that case, temperatures as well as the injected water flow were limited due to instability of the porous medium. Actually, fluidization phenomenon of the porous bed was also observed during tests nb81 (at 700 °C and 20 $m^3/h/m^2$ for Ø4mm, see Table 4, and nb95 (at 700 °C and 10 $m^3/h/m^2$ for Ø2mm, see Table 5). In these experiments, the power deposition was limited at 70 W/kg due to the lower efficiency of the inductive process with the small particles.

Table 6 Test matrix – 4th campaign (particles size of Ø 1 mm)

Test reference	Temperature	Power deposition	Flow water rate
98 D180 B1Q4 T200	220 °C	70 W/kg	1 $m^3/h/m^2$
99 D180 B1Q4 T300	320 °C	70 W/kg	2 $m^3/h/m^2$
100 D180 B1Q4 T400	420 °C	70 W/kg	2 $m^3/h/m^2$
101 D180 B1Q4 T300	320 °C	70 W/kg	4 $m^3/h/m^2$
102 D180 B1Q4 T400	420 °C	70 W/kg	4 $m^3/h/m^2$
104 D180 B1Q4 T400	420 °C	70 W/kg	5 $m^3/h/m^2$
105 D180 B1Q4 T400	410 °C	70 W/kg	7,5 $m^3/h/m^2$
106 D180 B1Q4 T700	700 °C	70 W/kg	5 m3/h/m2

Experiments at higher power will be completed using a "25kW/400kHz" HF generator. These series ended with the observation of the debris bed instabilities at lower injected flow rate (5 m3/h/m2 at 700°C and 7,5 m3/h/m2 at 400°C) compared to that observed with the Ø2 and Ø4 mm particles.

5. Experimental results

It is worth to compare the PRELUDE experiments with experiments made at Brookhaven National Laboratory by Tutu in the 80's [6]. Compared to these experiments, PRELUDE tests have brought complementary measurements with a specific attention on reproducibility: tests performed have shown that disturbances observed in some measurements (in particular perturbations on temperature recorded during the reflooding) are not produced randomly but are reproduced for every test. This makes us confident in the use of experimental data.

5.1 Experimental procedure

The debris bed, starting from room temperature, is brought to its initial temperature (200 to 900°C) by inductive heating with a specified power deposition (Figure 5) that is maintained during the reflooding. The heat up phase lasted about 1 hour for experiments at 700°C, because of the thermal losses of the experimental device. The liquid water is injected at about 20°C at the bottom of the debris bed. The constant water flow rate is obtained by pressurization of the upper plenum of the "water tank" by nitrogen. Typical temperature distributions in radial and axial directions, shown in Figure 10 (t0), are rather homogeneous, except at the periphery of the debris bed. During reflooding, temperature, flow rate and pressure were recorded at intervals of 0,1 s. The water flow was stopped after the complete quenching of the debris bed.

5.2 Temperature measurements

Figure 6 gives an example of the temperature evolution (as function of elevations and radial positions) during the reflooding phase (inlet water: 5 $m^3/h/m^2$) on a debris bed with particles of Ø4mm.
At a given location, quenching of thermocouples located in the pores (in the porosity of the debris) is faster than quenching of thermocouples inside the particles.

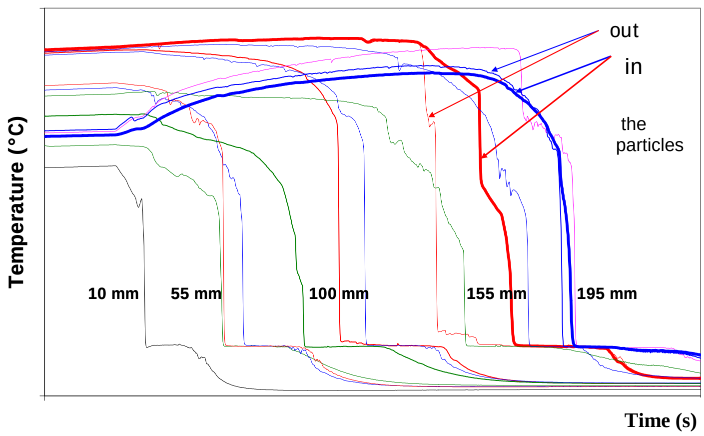

Figure 6: Typical temperature measurements

Thermocouples inside the debris bed allowed a fine view of the different phases of the transient and are useful to follow the front quench propagation. The measurements of temperature are accurate enough to derive the heat fluxes in the different regimes during the reflooding phase for modelling purpose.

5.3 Mass flow rate and pressure drop measurements

The measurements of the injected water flow (Figure 7), as well as the steam flow rate generated during reflooding were accurately obtained by means of accurate sensors to reach a very satisfactory mass balance (error around 120g : roughly 2 %).

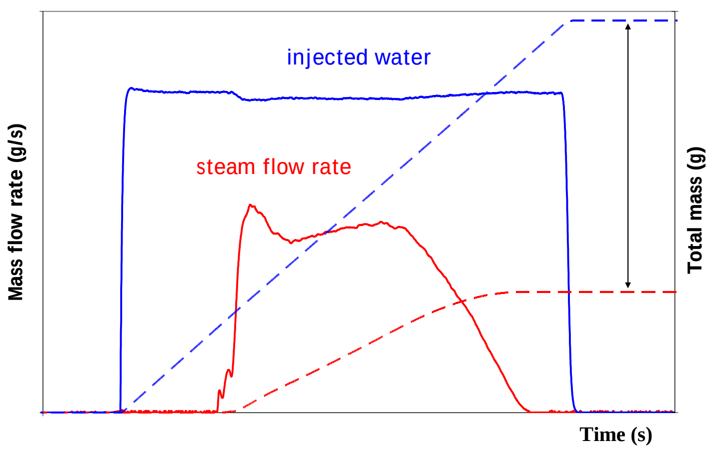

The difference between the cumulated water injected and steam production during the reflooding (roughly 6150 g) is consistent with the total water amount remaining the test section obtained by weighing (6270 g). During the reflooding, about 60% of the water injected was converted into steam, value which is in rather good agreement with the ICARE-CATHAREV2 pre-tests calculations.

Figure 7: Typical water/steam flow rate measurements as function time

Figure 8 illustrates the pressure drop across the debris bed during the reflooding.

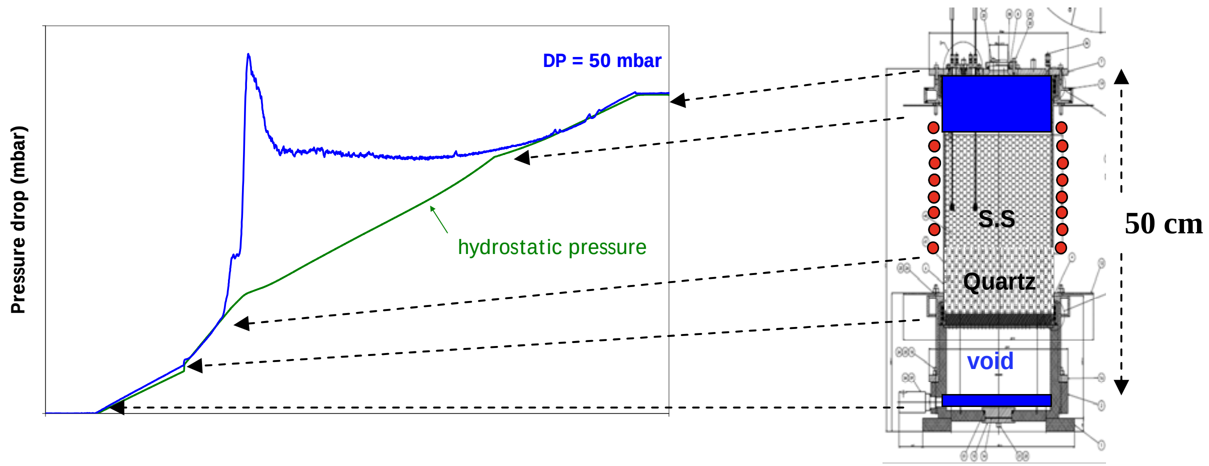

Figure 8: Pressure drop measurement across the debris bed as function time

The calculation of hydrostatic pressure ($\rho_w g\ h$) was deduced from the evaluation of the water front propagation which was estimated from the volume occupied by the remaining water in the test section (Q injected – Q steam released) as a function of time. It is assumed that the two-phase region has a negligible thickness.
The analyses of all the results concluded that pressure drops (ranging from 10 to 200 mbar depending on steam mass flow rate) in the debris increases as the particles size decreases (from Ø4 to Ø1mm), as foreseen due to permeability and passability changes.

5.4 Analysis of the water front propagation during the reflooding

The analysis of those preliminary results (Figure 9) outlined specific 2D effect during the reflooding with preferential propagation of the water at the peripheral part of the debris bed where temperatures are lower due to thermal losses and larger porosity (Figure 10- t0).
This phenomenon was enhanced for the smallest particles due to the lower permeability of the debris bed (see sub-section 5.5.2).

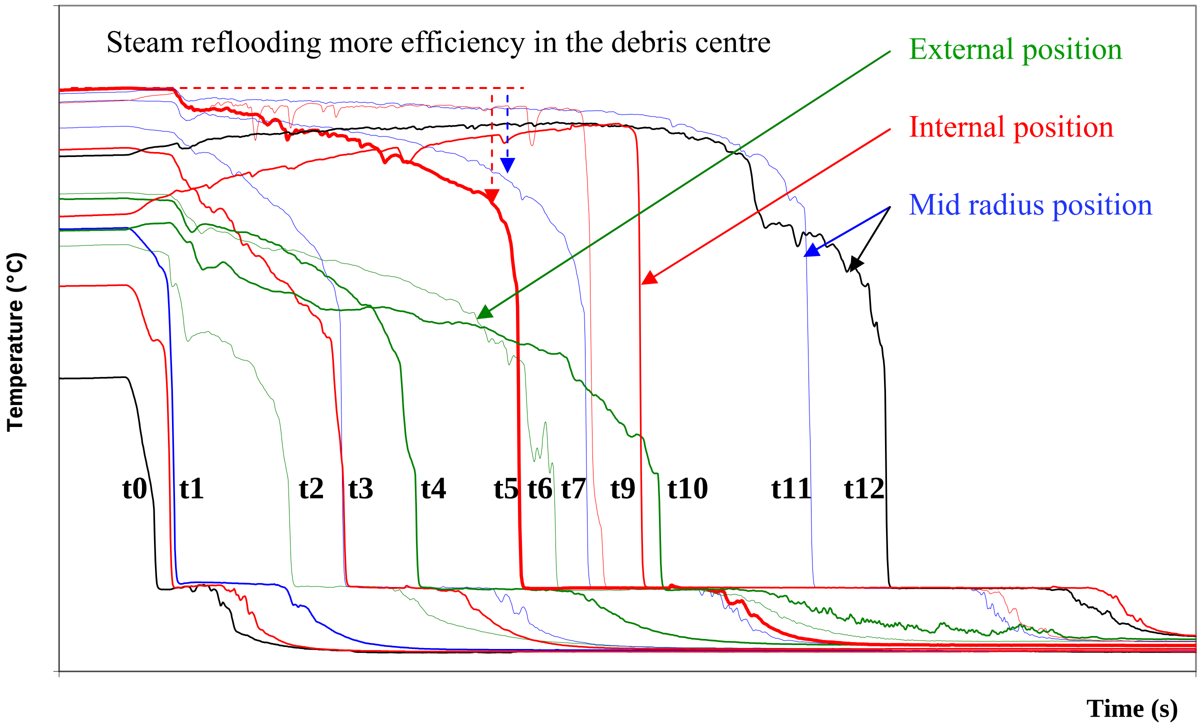

Figure 9: temperature evolution during reflooding at high injected flow rate

The temperature maps as function of time illustrates rather well the 2D aspects of the reflooding with a relative high flow rate (Figure 10).

When the water reaches the bottom of the debris bed, the quenching is observed for all the radial location (Figure 10 at t1). Then the quench front propagates upwards prior at the periphery (Figure 10 - t3, t4 and t5). One can observe a second preferential penetration of the water in the middle part of the debris bed (Figure 10 - t5 to t10): this may be the consequence of the decrease of the temperature during the first phase of the reflooding due to the stronger production of steam in the lower and middle part of the debris (the steam reflooding seems to be more efficient in the centre and in the middle height of the debris – see the observation on the Figure 9). This behavior has been already observed in the Tutu experiments [6].

o : thermocouples positions

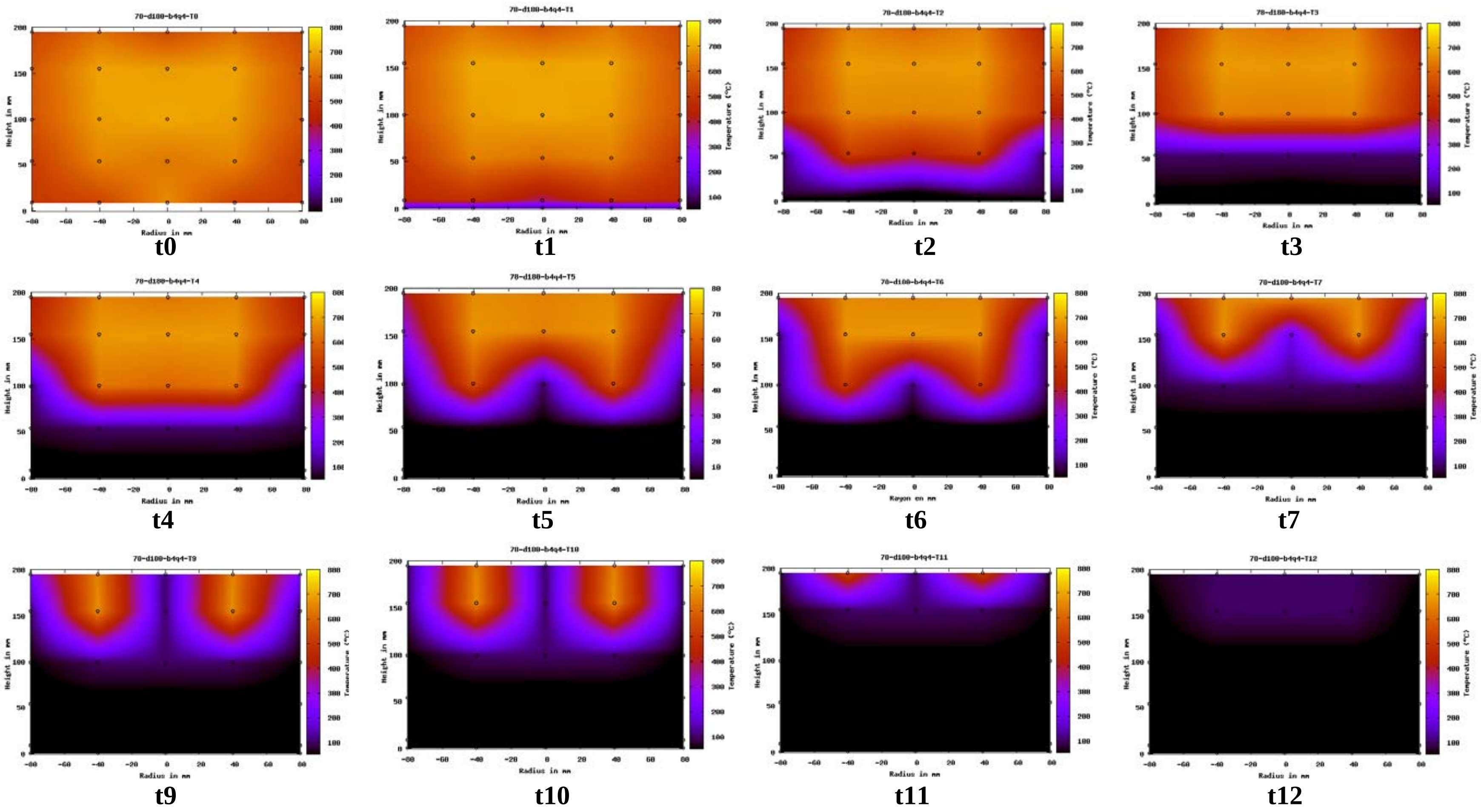

Figure 10: temperature maps as function of time during the reflooding

At higher flow rate (beyond 10 m/h), the water front propagation is so fast at the periphery that the liquid water arrives at the top while the core of the debris bed is not completely quenched leading to simultaneous bottom and top reflooding. This process that could lead to complex 3D thermal hydraulics behavior will be enhanced in the case of the large scale PEARL experiments including the core bypass simulated by non heated quartz spherical particles.

5.5 Sensitivity studies on thermal hydraulic parameters and morphology of the debris

Parameters to be tested in the large scale PEARL experiments are the initial temperature of the debris bed (up to 1000°C), the system pressure (1, 2, **3**, 5 and 10 bar), the inlet water superficial velocity (2, 5, **10**, 20 and 50 $m^3/h/m^2$), the injected water temperature (sub-cooling: 0, 20 and **50K**), the power deposition (100, **200** and 300 W/kg) and the particle size (1, 2, **3**, 4 mm diameter) representative of the nuclear reactor accident sequences. Some of those parameter ranges could be tested in the PRELUDE facility.

5.5.1 Debris bed initial temperature and inlet water superficial velocity

Figure 11 gives an example of the effect of the inlet water velocity for two series of experiments performed with a debris bed (Ø4 mm particles size) at 400 and 700°C.

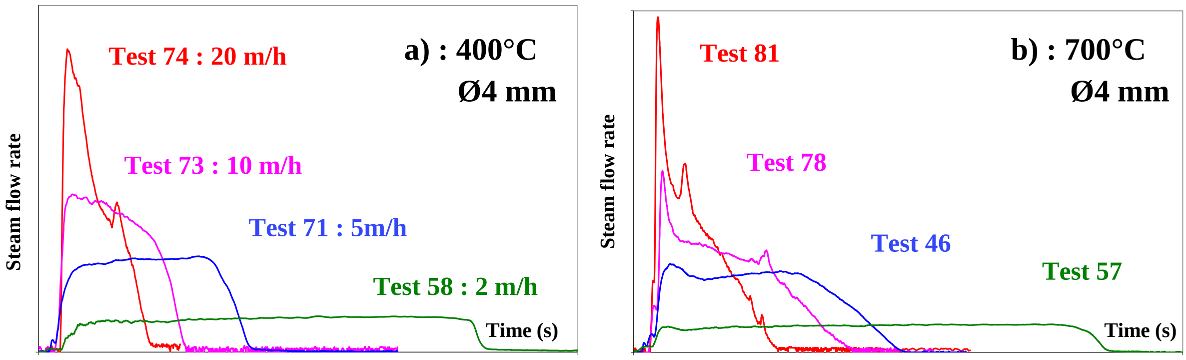

Figure 11: Flow rate (time) - Effect of inlet water velocity: 2, 5, 10 and 20 m/h (400/700°C)

The duration of the reflooding phase and the steam flow rate are strongly linked to the injected water superficial velocity. Using a very low flow, the production of the steam reaches rapidly a rather constant production of steam, whereas the high flow rate produces at the beginning of the reflooding, a pronounced peak of steam production. The very high steam velocity (evaluated to be about 20 m/s in the upper plenum for the test 81) leads to instability of the debris bed due to fluidization (spouted beds pattern as foreseen in the literature – Reh diagram [15]).
This phenomenon should be avoided for the larger scale PEARL experiments, in order to maintain a fixed geometry for modelling purpose [14] and to keep the instrumentation available for several experiments.
To summarize, the detailed analyses of the thermocouples lead to reflooding configurations with different flow patterns:

- At small injection rate, the quench front is approximatively flat, travelling with a constant velocity (1D behaviour of the front). The steam flow rates leaving the top of the debris are constant during the quenching process for various initial temperatures (400 and 700°C),
- At higher injection rates, the quenching process becomes 2D (complex geometry of the quench front) and the steam flow rate presents a peak shape at the beginning of the quench (behaviour enhanced with the increase of the initial temperature of the debris bed). Tutu [6] has an explanation that the peak behaviour at higher injection velocities can be explained by an extended quench region (instead of a thin quench front).

The same behaviours were observed (Figure 12) with others particle sizes (Ø2 and Ø 1 mm).

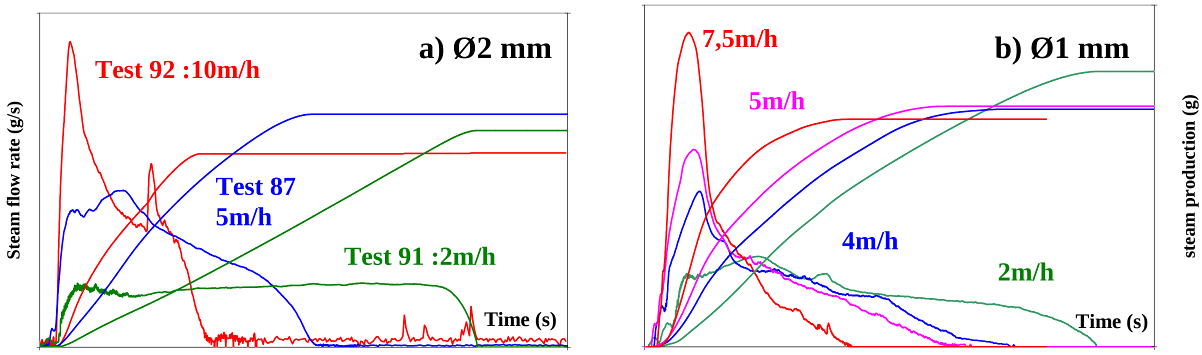

Figure 12: Effect of inlet water velocity (at 400°C) for 2 particle sizes

The slight lower amount of steam production (Test 92 – Figure 12a) is due to the fact that two phase release in the outlet circuit was observed for the second part of the reflooding phase: relation to determine steam flow rate, only available for single phase, could give wrong data.
At high flow rate (10 m/h) liquid water is transported in the upper plenum by the periphery of the debris bed, while steam is still produced to quench the inner part of the porous medium. Liquid water is then transported by drag forces in the outlet line (as droplets) due to the steam velocity. In addition, part of the produced steam is condensed by the upper water and therefore the steam released is lower than in the previous case (2 and 5 m/h). This behaviour is observed during the test 92 (as for tests 81 and 74 – cf § 5.5.1), with high flow rate by analysing thermocouples located in the upper plenum and in the steam outlet line (reaching the saturation condition indicating the presence of two phase flow). This problem for steam flow measurement will be enhanced in the Top Quench experiments foreseen in the PEARL facility.

5.5.2 Debris bed initial temperature and particles size

Figure 13 illustrates temperature evolutions during the reflooding for different particle sizes (Ø4, Ø2 and Ø1 mm) for a debris bed initial temperature around 400°C with a constant injected water velocity (5 $m^3/h/m^2$). Reflooding is more difficult as particle size decreases which impacts the duration for a complete quenching of the debris bed. With constant water injection in principle the same amount of water is penetrating the bed, independent of the particle size. The point is that with decreasing particles sizes the two-dimensional effects become stronger and quenching takes longer in the centre (but is faster in the periphery). In a final phase, water could bypass through already quenched regions and does not contribute to cooling any more.

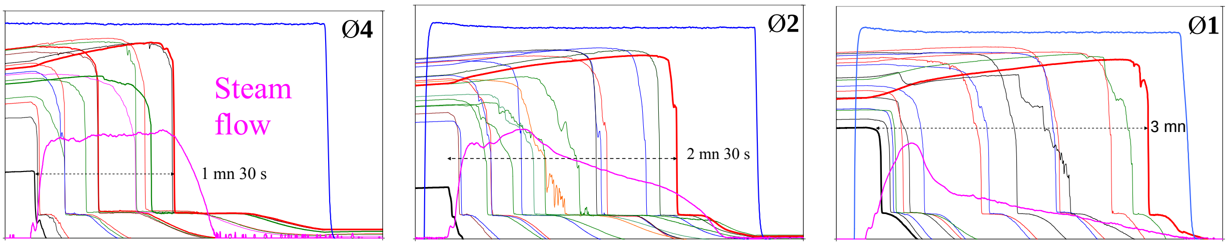

Figure 13: Temperature (time) - Effect of particle size - 4, 2 and 1 mm (5 m/h from 400°C)

The duration of the reflooding phase (i.e. time until quenching of the whole bed) is longer (double time) for the smallest particles. One can also observe the progressive change of the time profile of the steam flow, from constant rate (Ø4) to peak and decrease (Ø1), indicating modification of front quench propagation pattern.

Figure 14 illustrates the effect of particles size on the steam production during the transient.

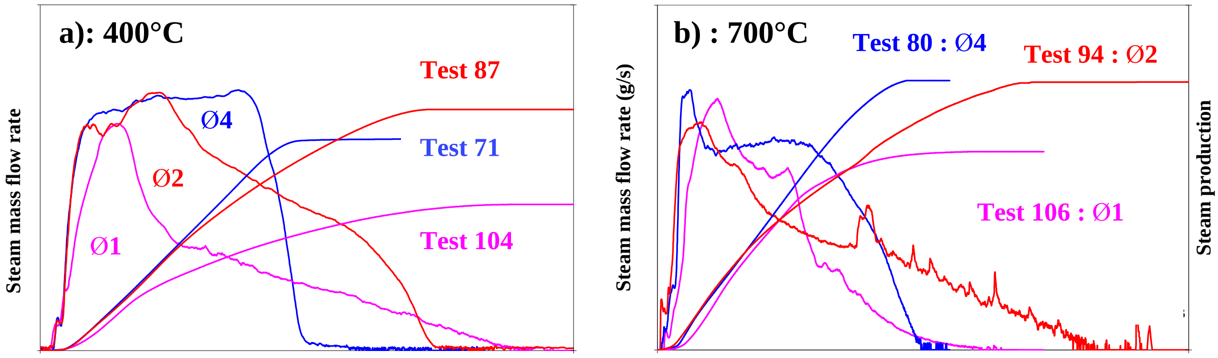

Figure 14: Flow rate (time) - Effect of particle size - 4, 2 and 1 mm (at 400 and 700°C)

The lowest value of the total amount of steam production with the smallest particles (Figure 14a) is partly due to the lowest value of power (70W/kg instead of the nominal value of 200 W/kg in the previous tests) and the lower efficiency of the reflooding (due to bypass phenomenon). At 700°C, contrary to what has been outlined above, the quenching seems to be faster with the smallest particles size (Figure 14b), probably because of fluidization. This phenomenon is well known, in the industrial processes, to increase the heat transfers inside a porous medium. The fine analysis of all the results regarding that phenomenon will be used to clearly define a domain for the thermal hydraulic conditions of the PEARL test matrix to avoid that configuration, in particular for bottom quench experiments compared to top quench experiments.

6. Conclusion

To address the damaged core coolability issue, an experimental program devoted to the analysis of debris bed reflooding has been launched at IRSN. A step-wise approach has been adopted, with feasibility and preliminary reflooding tests in the PRELUDE facility before doing more complex and representative tests in a larger PEARL facility to address the multi-dimensional thermal-hydraulic processes involved in reflooding situations in a nuclear reactor during severe accident. The preliminary experimental program started in 2009 to test the performance of the induction heating system of stainless steel particles simulating the debris bed and the instrumentation (temperature, pressure, water and steam flow rates), for an optimized design of the PEARL facility. Reflooding experiments were performed in PRELUDE, at atmospheric pressure using an Ø180mm test section diameter, 200mm height including 24kg of slightly oxidised amagnetic stainless steel Ø4, Ø2 and Ø1mm particles. This campaign provided heating sequence of a debris bed at about 200W/kg up to 700°C before the bottom water injection, with water flow rate range representative of reflooding of a nuclear reactor.

Those preliminary results provide accurate measurements for modelling purpose [16].

These results obtained at 1 bar will be extended in 2011 and 2012 with reflooding experiments with higher (500mm height) and larger (250mm height, Ø290mm with bypass) tests sections (<60 kg) on a homogenous debris bed up to 1000°C as well as on heterogeneous porous media (mixture of particles of different diameters and non spherical particles).

Results thus provided on PRELUDE facility have helped to optimize the design of the PEARL facility under construction in 2011, in order to run experiments from 2012 on larger debris bed (500kg, Ø540mm, 500mm height) at higher pressure up to 10 bar.

7. References

[1] J-P. Van Dorsselaere, F. Fichot (IRSN), J-M. Seiler (CEA), "Views on R&D needs about in-vessel reflooding issues, with a focus on debris coolability", Nuclear Engineering and Design 236 (2006), pp.1976–1990

[2] M. Bürger, M. Buck, G. Pohlner, S. Rahman, R. Kulenovic (IKE), F. Fichot (IRSN), W.M. Ma (KTH), J. Miettinen, I. Lindholm (VTT) and K. Atkhen (EDF), "Coolability of particulate beds in severe accidents : Status and remaining uncertainties", Progress in Nuclear Energy, Vol. 52, 1, pp. 61-75, 2010

[3] N. Stenne, F. Fichot, J.P. Van Dorsselaere (IRSN), W. Tromm, M. Steinbrueck, J. Stuckert (KIT), M. Buck (IKE), "Multi-Dimensional Reflooding experiments: the PEARL Program, Joint OECD/NEA" - EC/SARNET2 Workshop "In-Vessel Coolability , Issy-les-Moulineaux, France, October 12-14, 2009

[4] N. Stenne, F. Fichot, JP. Van Dorsselaere (IRSN), W. Tromm, M. Steinbrueck, J. Stuckert (KIT), M. Buck (IKE), R&D on reflooding of degraded cores in SARNET- Focus on PEARL new IRSN facility, *EUROSAFE Forum*, Brussels (Belgium), Nov.2-3, 2009

[5] F. Fichot, G. Repetto, O. Coindreau (IRSN), M. Steibruck W. Hering (KIT), M, Buck, M. Burger (IKE), "Understanding the effects of reflooding in a reactor core beyond LOCA conditions", 4th European Review meeting on Severe Accident Research (ERMSAR-2010), Bologna, Italy, May 11-12, 2010

[6] Tutu, et al., "Debris bed quenching under bottom flood conditions", Report NUREG/CR-3850, Sandia National Laboratory, 1984

[7] T. Ginsberg, J. Klein, J. Klages, Y. Sanborn, C.E. Schwarz, J.C Chen, L. Wei, "An experimental and analytical investigation of quenching of superheated debris beds under top-reflood conditions"- Tech. report NUREG-CR-4493. Sandia National Lab, 1986

[8] CH. Wang and V.K. Dhir, An experimental investigation of multidimensional quenching of a simulated core debris bed, Nuclear Engineering and Design, 110 (1988), pp. 61-72

[9] M. J. Konovalikhin, and B. R. Sehgal, Investigation of volumetrically heated debris bed quenching, Proceedings of ICONE-9 Conference, Nice, France, April 8–12, 2001

[10] K. Atkhen and G. Berthoud, "SILFIDE experiment: Coolability in a volumetrically heated debris bed", Nuclear Engineering and Design. 236 (2006), pp. 2126-2134

[11] I. Lindholm et al, “Dryout heat flux experiments with deep heterogeneous particle bed “, Nuclear Engineering and Design, 236 (2006), pp. 2060–2074

[12] P. Schäfer, M. Groll and R. Kulenovic, “Basic Investigations on Debris Cooling“, Nuclear Engineering and Design, 236 (2006), pp. 2104-2116

[13] O. Coindreau et al., Characteristics of the geometry of a severely damaged core and of the debris bed expected to form during reflooding, Joint OECD/NEA“ - EC/SARNET2 Workshop “In-Vessel Coolability , Issy-les-Moulineaux, France, October 12-14, 2009

[14] A. Bachrata, F. Fichot, G. Repetto, J. Fleurot (IRSN), M. Quintard, “Reflooding of a severely damaged reactor core experimental analysis and modeling”, Proceedings of ICONE-9 Conference, Chiba, Japan, May 16-19, 2011

[15] L. Reh, “Fluid bed processing”, Chem. Engng. Prog., 67, pp. 58-63 (1971)

[16] A. Bachrata, F. Fichot, G. Repetto, J. Fleurot (IRSN), M. Quintard, “Quench front progression in a superheated porous medium: experimental analysis and model development”, (NURETH14), Toronto, Canada, September 25-29, 2011

ACKNOWLEDGMENTS

Part of this work was performed within the framework of the SARNET2 Network of Excellence of the 7th European Framework Program. The authors gratefully acknowledge funding by Euratom to support this activity.